World Academy of Science, Engineering and Technology
International Journal of Mechanical and Mechatronics Engineering
Vol:9, No:5, 2015

3D Finite Element Analysis for Mechanics of Soil-Tool Interaction

A. Armin, R. Fotouhi, W. Szyszkowski

***Abstract*—**This paper is part of a study to develop robots for farming. As such power requirement to operate equipment attach to such robots become an important factor. Soil-tool interaction plays major role in power consumption, thus predicting accurately the forces which act on the blade during the farming is very important for optimal designing of farm equipment. In this paper, a finite element investigation for tillage tools and soil interaction is described by using an inelastic constitutive material law for agriculture application. A 3-dimensional (3D) nonlinear finite element analysis (FEA) is developed to examine behavior of a blade with different rake angles moving in a block of soil, and to estimate the blade force. The soil model considered is an elastic-plastic with non-associated Drucker-Prager material model. Special use of contact elements are employed to consider connection between soil-blade and soil-soil surfaces. The FEA results are compared with experimental ones, which show good agreement in accurately predicting draft forces developed on the blade when it moves through the soil. Also a very good correlation was obtained between FEA results and analytical results from classical soil mechanics theories for straight blades. These comparisons verified the FEA model developed. For analyzing complicated soil-tool interactions and for optimum design of blades, this method will be useful.

***Keywords*—**Finite element analysis, soil-blade contact modeling, blade force.

I. Introduction

THE motivation of this study is to develop autonomous vehicles for agricultural setting to help farmers in crop production. Soil-tool interaction, especially tillage, is a procedure of preparing the soil for seeding. About half of energy used for crop production is consumed by tillage operation because of high draft force on tillage as [1] stated. This high energy consumption is not only because of the motion of large amount of soil mass, but also because of inefficient methods of energy transfer to the soil as [2] stated. All soil-tillage interaction researches have been focused to develop force prediction models by using different kinds of soil (soil physical and mechanical characteristics), tool (tool shape, tool's rake angle), and operating conditions (depth of cut, width of cut, travel speed, etc.) as [3] stated. Since blade shapes affect the shape and size of the soil failure one and consequently forces on the blade, optimization of the tillage-tool design will help to improve energy efficiency. Due to the complex nature of the system, prediction of forces in analytical models is limited to simple rectangular blades shape. Therefore, analytical method cannot provide enough information for optimum design of a tillage-tool. Improvement in computers and computational techniques has led to the development of a new generation of highly efficient programs for simulating real situations with several parameters as [4] stated. Numerical techniques, especially finite element method (FEM), help to analyze the soil–tool interaction with the development of a suitable constitutive (stress-deformation) relation for specific working condition. FEM can be used to predict information about the failure zone, field of stress, soil deformation, acting forces on blades for agricultural equipment without limitation on the shape of blades. There are several models have been done based on finite element analysis (FEA), such as [5]-[8]. In these research works, they proposed different types of FE models to simulate soil-tool interaction and to obtain response of tools during these interactions.

From the numerical viewpoint soil separation is somewhat similar to the problem of cutting chips in machining operations [11]-[13], where various geometrical and physical separation criteria were developed based on critical values of displacements, strains, stresses, or strain energy to estimate the beginning of separation. A new criterion that uses the limit compacting strains in the direction of cutting is proposed here. When using this criterion to the FE model the soil particles are separated 'discretely' at consecutive nodes starting from the node that is nearest to the cutting edge of the blade.

The overall objective of this research work is to develop a simulation procedure for modeling the soil-tool interaction for arbitrary shape of the blade. Here the proposed procedure is tested on the straight blades in order to compare it with available analytical/experimental results [9], [10]. In particular, the use of contact elements, modeling sliding and cutting as the blade moves through the soil is explained in detail, as well as the method of calculating the draft force for the separation process that in fact takes place discretely at successive nodes. The soil selected for this study is the type of soil commonly found in Saskatchewan.

II. Constitutive Law for Soil

In this research, the soil-blade interaction is modeled by the Drucker-Prager criteria with a non-associate flow rule controlled by the value of dilatancy angle v, which represents the volumetric expansion and frictional-dilatancy behavior of the material. If there is no volumetric expansion, then $v = 0$ (shear type of deformation only), which corresponds the direction 3 (vertical) of the increments of plastic strain in Fig. 1. On the other hand, for the flow rule associated with criterion (1) the increments of plastic strains would have direction 1 that contains shear deformation and dilatations

Ahad Armin is with the Red Deer College, Canada (e-mail: ahad.armin@rdc.ab.ca).

characterized by the dilatancy angle $v = \varphi$. According to [14] for real materials angle v is usually less than φ and should be within the limits $0 < v < \varphi$ as indicated by direction 2 (the values of parameters used in the paper are listed in Table I).

In the numerical analysis with the external load increasing a typical material behavior defined by this law is plotted with dotted curve. It starts with elastic deformations until the yield criterion is reached and then the curve lines up with the yield surface (points are on this surface). Plastic deformations generated along the yield surface may be considered as compacting.

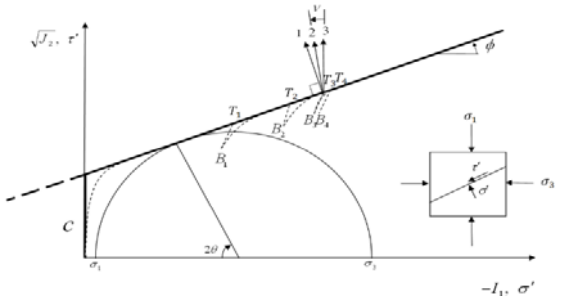

Fig. 1 The Drucker-Prager material law with non-associated flow rule

Since the separation status in FE can only be defined at nodes, the simulated separation process is 'discrete' in this sense that there would be some stress relieve when the status at a particular node is changed from initially connected to separated. For example if just before the first separation the stress state is defined by T_1 then just after separation it will be lowered and back in the elastic region. In this region the highest stress state, defined by B_1, will be typically at the opening's tip, i.e. at the node to be separated next. Then after a further load increase (controlled here by the forced blade's displacement) the stress state is observed at the node that would separate next. This stress state must first reach the yield surface again and then followed it until arriving at point T_2 where the separation criterion is met again. After separating at the subsequent node the stress state drops to B_2, and so on (points B_1, B_2 are further interpreted, discussed and shown in Fig. 4).

III. Material and Methods

A. The FE Models

In the FE general 3D model both soil and blade are represented by the hexahedral elements SOLID45 from the ANSYS [15] library of elements, which have 8 nodes and 3 degree of freedoms (DOF) at each node. The soil-blade connection is modeled by the contact elements CONTACT173 and TARGET170 placed along the separation surfaces as discussed in the next section. The model with the elasto-plastic constitutive law, the separation procedure, and with elastic incisions (see Fig. 1) require a relatively large number of equilibrium iterations for convergence, therefore the calculations are generally long (typically lasting several hours). Therefore a number of meshing patterns (with high mesh density near the contact areas) were tried for balancing computational effort with accuracy of calculations.

B. Model Description

Geometry of the 3D model is sketched in Fig. 2. The model is parametric with several parameters defining the geometry of soil and tool. The soil block is L_S= 300mm long, w_S= 300mm wide, and d_S= 150mm deep. These dimensions were selected in such a way that the solution in the vicinity of the blade is not sensitive to the block's size. The block is divided into sub-blocks that can be meshed with different mesh densities. The maximum distance blade can travel while cutting the soil, also the length of contacts between upper and lower blocks of soil, is L_f= 50mm (this dimension will be justified later). Parameter w_1 is the width of cut soil (also the width of blade), w_2 is the side width of soil block. The depth of cut soil is d_1; which is also the cutting depth of blade. Tilting of the blade with respect to the soil is defined by α, the rake angle.

TABLE I
Soil and Blade Parameters Used in Present Analysis

Properties	Soil	Blade
C- Cohesion	$20Kpa$	
φ- Soil internal friction angle	35°	
v - Dilatancy angle	20°	
$\bar{\omega}$- Soil water content	7%	
E - Modulus of elasticity	5 Mpa	200000 5 Mpa
μ - Poisson's ratio	0.36	0.3
ρ - Density	$1220\frac{Kg}{m^3}$	$7850\frac{Kg}{m^3}$
φ_b - Blade-soil friction angle	23°	

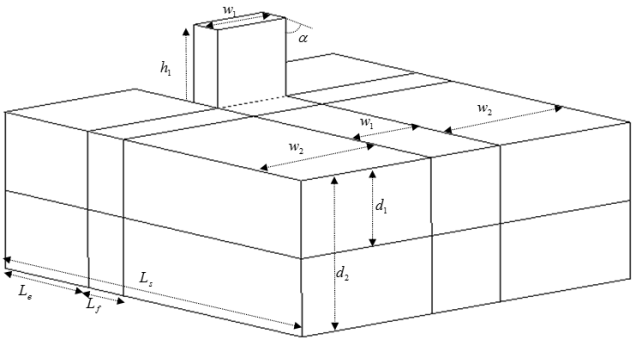

Fig. 2 Geometrical parameters of the FE model

The starting point of blade's travel inside the soil block is denoted by L_e= 50mm+$d_1 cos\alpha$. The blade's total height is h_1 = 100 mm. This parameter does not affect the cutting process. The ranges of d_1 = 25- 50mm, w_1= 20-160mm, and α = 30-90° were examined.

C. The Soil-Blade Interaction

The soil is in contact with the blade on four surfaces shown in Fig. 3. The soil separation takes place along surfaces 1 and 3 (the vertical cuts) and along surface 2 (the horizontal cut). These surfaces will be referred to as the separation surfaces, and the contact elements with bonding and sliding options are used to model these connections. On surface 4, however, the soil should be allowed to slide along the blade without

separation. Therefore the contact elements with only sliding option should be used there. This surface will be referred to as the sliding surface.

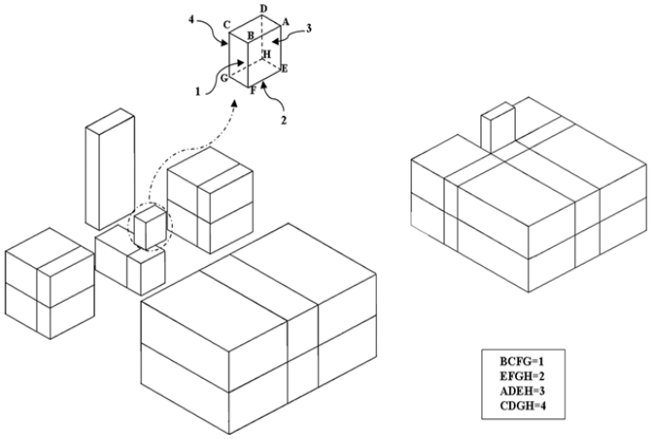

Fig. 3 The surfaces with contact elements (bonding and sliding on surfaces 1, 2, 3, sliding on surface 4)

It should be noted that the separation surfaces are parallel to the direction of the blade's motion, while the sliding surface is parallel to the front of blade. For the numerical purposes the separation and sliding surfaces are actually modeled by two surfaces connected via the contact elements (and initially the nodes belonging to these two surfaces coincide). Any relative soil motion takes place on these surfaces during the soil-blade interaction.

The separation process is similar to the process of cutting chips in machining operations [11]-[13] or to the crack propagation process, i.e. there is always a small crack moving in front of the blade that allows the blade to travel through the soil (such a crack can be observed on the deformation pattern shown in Fig. 5). The nodes on the separation surface can move apart if a specified separation criterion is met. The distance u traveled by the blade's tip is measured from L_e, and its maximum value is L_f .

D. The Separation Criterion

The elements above and below the expected separation surface are connected at nodes using the contact elements that allow to activate or deactivate the bonding forces between them. The highest stress/deformation level is observed always in the element which is at the tip of the opening and is of a particular interest during the whole simulation. At the beginning all bonding forces are active and this element (to be referred to as the tip element) is adjacent to the tip of blade. As the blade starts to move, stresses go through the elastic phase (see the broken line in Fig. 1) until the solid line representing the yielding condition (1) is reached (where the Drucker-Prager plasticity rules are followed). In the tip element the strain component ε_x (in the direction of the blade's motion) is monitored continuously. The elasto-plastic process will continue until ε_x reaches a predefined magnitude of ε_c (which may be referred to as the limiting compacting strain) with the stress state reaching point T_1 in Fig. 1. At this instant the force bonding the nodes at the opening's tip (of the tip element) is deactivated, and the node separate generating the first opening of length equal to the size of the element's side. This is also associated with the stresses being relieved to the state denoted by point B_1, which will again be inside the elastic range (i.e. inside the surface defined by the yielding condition), and a drop in the value of ε_x below ε_c. With the blade moving forward the stress state will be increasing to reach the yielding condition again but at the new tip of opening that is now away from the blade's tip. The strain ε_x will become equal to ε_c at T_2 and the node separate at this tip increasing the opening's length by the size of that element and causing the stress (and strain) relieve indicated by point B_2, and so on.

The numerical experimentations indicate that for this type of soil if $\varepsilon_c \approx 0.3$ then the resultant draft force (the procedure to determine this force is discussed in the next section) was best matching the results obtained from the 'engineering' formulas presented in [9], [10], and often used by the designers of tools for tillage operations. However the choice of limiting strain ε_c is dependent on internal friction angle. By increasing internal friction angle the value of limiting strain increases almost linearly.

Since the continuous process of cutting the soil is modeled 'discretely' (by disjoining consecutive nodes on the separation surface), the local stiffness in the vicinity of the opening's tip changes abruptly with the system appearing to be slightly stiffer before the separation and slightly softer after separation. Such effects will be taken into account in the next section that presents the method of calculating the draft force required to move the blade through soil.

The separation procedure also affects how the stress state in soil follows the Drucker-Prager criterion (1), which in the σ_1, σ_3 coordinates (i.e. in $\sigma_{min}, \sigma_{max}$ respectively and assuming σ_2 at the instant of separation) can be represented by ellipsoidal yielding curves growing or shrinking dependently on the magnitude of the current pressure. Such curves for soil are significantly affected by the internal friction φ, and generally shift towards compressive stress components.

E. Calculating Forces on the Blade

As already mentioned the analysis is quasi-static, the stress-strain states in the whole FE model are calculated for increasing horizontal distance traveled by the blade, u. The forces (draft and lift) acting on the blade are determined by properly integrating the stress components. The increments of u are assumed in steps (representing as the 'load' steps in ANSYS), which are larger between the separation instances and smaller around the separation. The size of each subsequent step can be estimated from the ε_x readings of the previous step. The values of such steps are quite important from the numerical viewpoint since too small steps may result in a substantial increase of the time of calculations.

For an assumed mesh size a typical calculated draft force depends on the distance traveled as shown in Fig. 4. The calculations start as elastic (OE range) with all the bonding forces active (and therefore all the soil elements still

connected), enter the plastic deformation at some point *E*, and then go to inelastic phase until deformation in the vicinity of the tip of the blade (point *A*) measured as ε_x , reaches the value of ε_c. This happens when the blade's displacement and the corresponding draft force reach the level defined as point T_1.

Then the bonding force in the first node is deactivated (or the elements above and below the separation plane closest to the blade are allowed to separate) that brings about a drop in the magnitude of the draft force to the value corresponding to point B_1 .

The opening equal to the element size along the separation surface is created and the stresses and deformation in its vicinity are reduced enough (see the explanations in the previous section) for the analysis to start at B_1 from an elastic level. Then first the yielding condition is reached, and next the instant when ε_x increases again to ε_c, which takes place at the blade's displacement and the draft force denoted by point T_2. Deactivating the bonding force in the second node bring the draft force to the level indicated by point B_2 (in the elastic range), and so on. The elements separated in the first and second deactivations are indicated with the broken lines.

Fig. 4 represents a typical relationship for the draft force versus the blade's displacement covering five separations (i.e. the cutting/opening runs through five elements) as obtained from the simulation.

Some details of the meshing and opening after three separations are shown in Fig. 5. One can note in the enlarged picture that the elements above the separation line have shrunk about 30% in the horizontal direction, which is the consequence of assuming $\varepsilon_c = 0.3$.

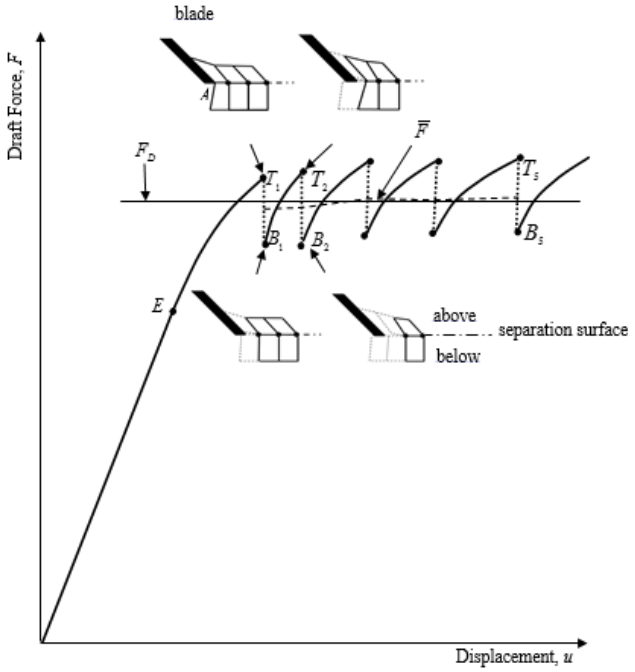

Fig. 4 The force developed on the blade using the first six elements in front of the blade

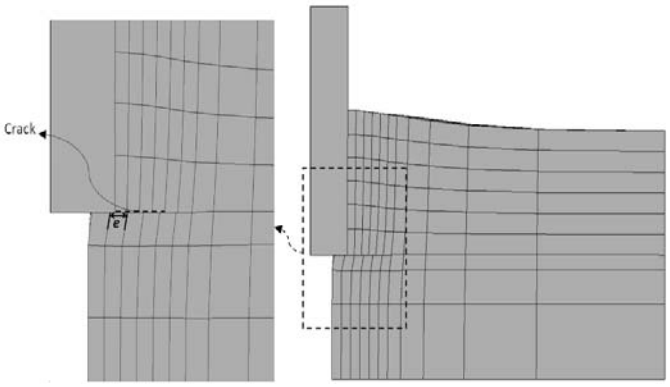

Fig. 5 The soil deformation after three separations (note the opening in front of the blade's tip)

The separation simulated by the FE model takes place sequentially at the nodes on the separation surfaces, as already discussed. When the bonding force at a particular node is deactivated the system suddenly changes its overall stiffness resulting in the draft force drop indicated by a jump $T_i - B_i$. It should be noted that in the 'discrete' modelling the separation force $F(T_i)$ is calculated for an underestimated length of the opening in front of the blade (i.e. shorter than for continues separation), and for an overestimated bonding force in the node to separate. Similarly, force $F(B_i)$ is calculated for an overestimated length of the opening and for an underestimated bonding force at the same node. Therefore one may interpret $F(T_i)$ as an upper limit of the draft force calculated continuously, while $F(B_i)$ as a lower limit of that force.

How much the draft force is over- and underestimated (or the difference ($F(T_i)$- $F(B_i)$) depends on the element size *e* on the separation plane (see Fig. 5). However, as our numerical experimentations will indicate, the average force $\bar{F} = [F(T_i)$- $F(B_i)]/2$ for *e* small enough appears to be essentially independent of meshing. Therefore it can be considered as an approximation of the draft force for the blade's displacement *u* at the instant of a particular separation. This force is plotted as a broken line, $\bar{F}$ in Fig. 4; note that it becomes almost constant even after one or two separation. Such a force is denoted by F_D, and it should represent the draft force to characterize the soil-tool interaction for particular conditions assumed in the simulation.

Since the shape of nonlinear portions $E - T_1$ and $B_i - T_{i+1}$ of the draft force-displacement characteristic are of less importance, the plots in the next sections will be simplified to show only points T_i and B_i (to demonstrate how they are getting closer with smaller *e*), and then $\bar{F}$ and the value of F_D.

F. Validation of the FE Model

For straight blades the following formula [10] is used for the draft force:

$$F_D' = (\gamma_s d_1^2 N_\gamma + c d_1 N_c + Q d_1 N_q) w_1 \quad (1)$$

where γ_s is soil specific weight, *c* is soil cohesion, *Q* is bearing pressure (due to soil accumulation), $d_1$is cutting depth of the

blade, w_1 is the width of blade (width of cut soil) and (N_γ, N_c, N_q) are tabulated cutting factors that depend on the soil friction angle φ, and the blade rake angle α. In our case, the last term is negligible, i.e. $Qd_1N_q \approx 0$, while the factors N_γ, N_c for the cases are: N_γ= 10.3, N_c = 22.0 for the blade with $\alpha = 90^\circ$, and N_γ = 4.94, N_c= 9.26 for the blade with $\alpha = 60^\circ$. Substituting into (1) one obtains F_D'= 893N for the case presented in Fig. 6 (0.4% difference with F_D= 896N of FEA results), and F_D'=470N for the case of $\alpha = 60^\circ$ (5.1% difference with F_D= 446N of FEA results). Using the proposed methodology the cases covering the range of d_1 =25-50mm, w_1 =20-160mm, and $\alpha = 30 - 90^\circ$ were simulated. In general, the differences between the simulated values F_D and the values F_D' calculated from (1) were typically about 2-3%, but never higher than 5%, which validates the methodology.

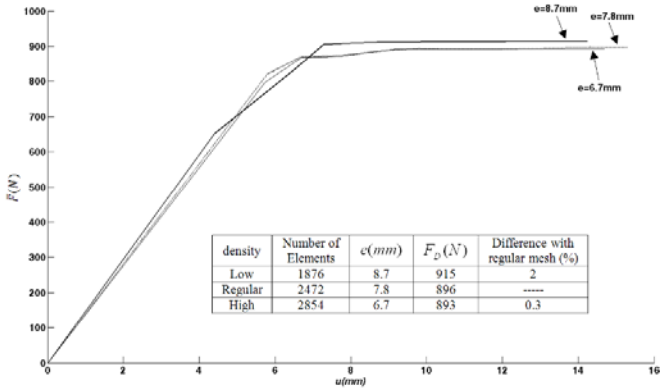

density	Number of Elements	$e(mm)$	$F_D(N)$	Difference with regular mesh (%)
Low	1876	8.7	915	2
Regular	2472	7.8	896	-----
High	2854	6.7	893	0.3

Fig. 6 Effect of e (and the mesh density) on the average draft force

IV. Some Deformation Results

The simulations rendered the deformation patterns that generally agreed with the expectations and what was described in [16], [17]. For the case in Fig. 6 the displacement in the z-direction when the blade is moved by about u = 16mm is presented in Fig. 7. The disturbed soil is accumulated in front of the blade and tends to swell up in upward and lateral directions with respect to its original configuration. Also as observed in [17] by moving blade through the soil in horizontal direction, each layer of soil (above separation surface) is pushed upward and accumulated soil can be described as a convex curve. It can be seen more clearly in Figs. 8 and 9.

The plastic strains in the X-Y plane of the blade's front for u = 16mm are plotted in Fig. 9. One can observe that these strains concentrate in a relatively narrow band inclined about $\theta \approx 29^\circ$ from the horizontal line. According to the simplified limit analysis this inclination should be $\theta = 45 - \frac{35}{2} = 27.5^\circ$ which is close to the value obtained from the simulation in FEA.

As shown in Fig. 10 by moving the blade, the soil around the moving blade is also goes upward to make an elliptical shape. By increasing in soil accumulation, the plastic strain on surrounding soil increase as well. The increased plastic strain based on soil accumulation is shown in Fig. 11 after blade moved 16mm in the horizontal direction. As it is shown in Fig. 11, the maximum plastic strain is on the top of the soil, adjacent to the blade; this (location of maximum plastic strain) is because of the soil deformation due to motion of the blade.

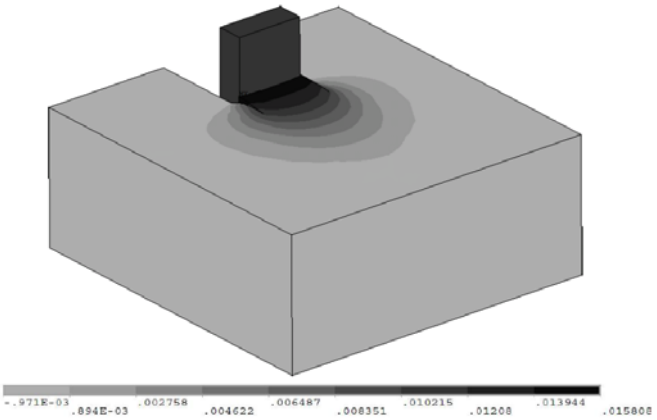

Fig. 7 The deformed shape and the displacement of soil in the horizontal direction

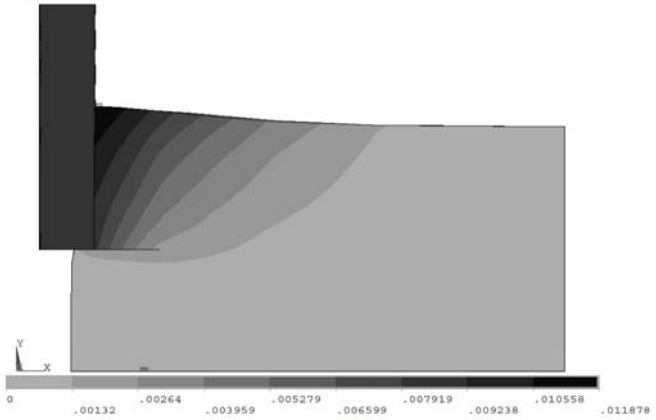

Fig. 8 Displacement of soil (in front of the blade only)

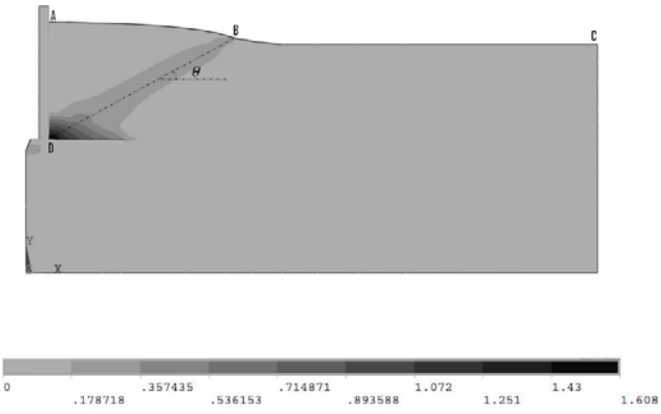

Fig. 9 Plastic strain distribution of soil in front of the blade ($\theta \approx 29^\circ$)

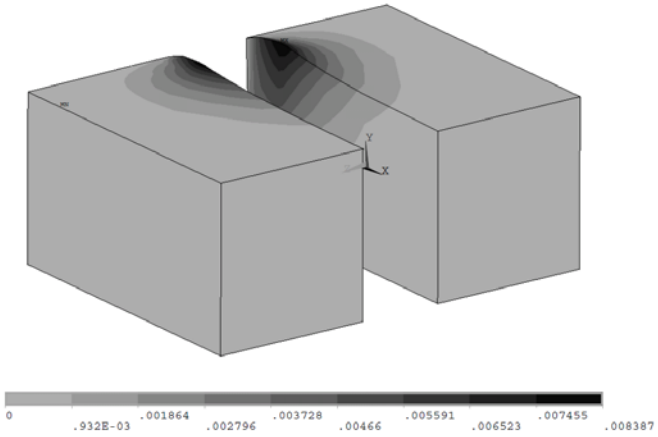

Fig. 10 Displacement of soil without the blade (blade moved 16mm)

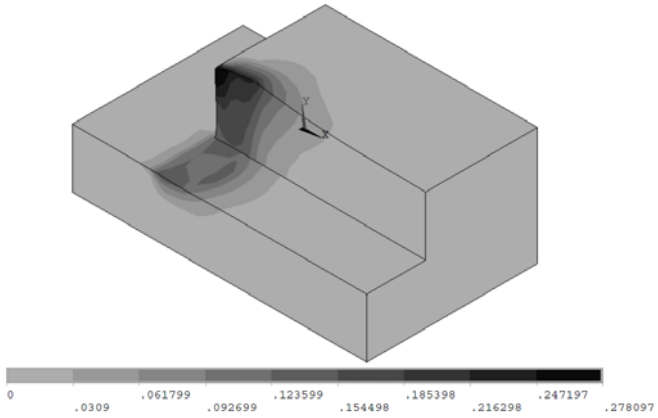

Fig. 11 Plastic strain distribution on the surrounding soil (blade moved 9mm)

V. Conclusion

A new procedure for simulating the soil-blade interaction by the Finite Element Method is presented. The procedure combines the non-associated Drucker-Prager constitutive law with a compaction strain based separation criterion to describe the behavior of soil while being cut by the blade. Several separation and sliding surfaces are defined and utilized in the analysis. The elements on these surfaces are bonded to each other by special use of contact elements. During motion of the blade through soil, the bonding along the separation surfaces is allowed to break resulting in separation of the soil elements in front of the blade. The sliding surfaces allow the soil to slide upward and sideways of the blade. A method of calculating the draft force that essentially eliminates the effects of 'discrete' disjoining particular nodes is proposed and tested for convergence.

The whole procedure is applied here to simulate the straight blades only, mainly for the purpose of validation. The simulation results appear to show a good correlation when compared with the semi-analytical formulas of the classical soil mechanics.

It is planned to extend the procedure's applications to the analysis of blades of arbitrary shapes, which in turn can be used in developing software for optimization of the tillage operations.

References

[1] Zhang, J., and Kushwaha, R.L. 1998, "Dynamic analysis of tillage tool: Part I – Finite element method", Canadian Agriculture Engineering; Vol (40), pp. 287-292.

[2] Ashrafi Zadeh, S.R, 2006. "Modeling of energy requirements by a narrow tillage tool'. Unpublished Doctoral Thesis at the University of Saskatchewan, Saskatoon, Canada.

[3] S.Karmakar, 2008, "Modeling of soil-tool interaction in tillage". Transworld research network, India.

[4] M. Abo-Elnor, R. Hamilton, J.T. Boyle, 2004, "Simulation of soil-blade interaction for sandy soil using advanced 3D finite element analysis", Soil & Tillage Research. Vol(75), pp. 61-73.

[5] J. Wang, and D. Gee-Clough, 1991, "Deformation and failure in wet clay soil. Simulation of tine soil cutting". Proc IAMC Conference Beijing, China. Pp. 219-226.

[6] L. Chi, and R.L. Kushwaha, 1989, "Finite element analysis of force on a plane soil blade". Canadian Agriculture Engineering, Vol(31), pp. 135-140.

[7] J. Shen, and R. L. Kushwaha, 1998, "Soil-Machine Interactions-A Finite Element Perspective", Marcel Dekker Inc. Publishers,.

[8] S.K. Upadhyaya, U.A. Rosa, and D. Wulfsohn, 2002, "Application of the finite element method in agricultural soil mechanics", Advances in soil Dynamics, PP. 117-153.

[9] D.R.P. Hettiaratchi, A.R., Reece, The calculation of passive soil resistance. Computers and Geotechnique. 24 (1974) 280-310.

[10] E. McKyes, O.S. Ali, The cutting of soil by a narrow blade. Journal of Terramechanics. 14 (1977) 43-58.J. Shen, and R. L. Kushwaha, 1998, "Soil-Machine Interactions-A Finite Element Perspective", Marcel Dekker Inc. Publishers,.

[11] J. M. Huang, J. T. Black, An evaluation of chip separation criteria for the fem simulation of machining. J. Manufacturing science and Engineering. 118 (1996) 461-469.

[12] Ng. Eu-Gene, D.K. Aspinwall, Modeling of hard part machining. J. Material processing technology. 127 (2002) 222-229.

[13] A.P. Markopoulos, Finite element method in machining process. Springer, London, 2013.

[14] Y. Chen, L. J. Munkholm, T. A. Nyord, Discrete element model for soil-sweep interaction in three different soils. Soil & Tillage Research. 126 (2013) 34-41.

[15] Ansys version 11.0: Standard user's manual, 2008. Available from www.ansys.come

[16] E. McKeyes, Soil cutting and tillage. Elsevier Science Publishing Company, New York, 1985.

[17] I. Shmulevich, Z. Asaf, D. Rubinstein, Interaction between soil and a wide cutting blade using the discrete element method. Soil & Tillage Research. 97 (2007) 37–50.